2021 IEEE Intelligent Vehicles Symposium (IV)
July 11-17, 2021. Nagoya, Japan

Evaluation of Macroscopic Fundamental Diagram Transition in the Era of Connected and Autonomous Vehicles*

Mohammad Halakoo[1] and Hao Yang[2]†, *Member, IEEE*

***Abstract*— The introduction of connected and autonomous vehicles (CAVs) could bring practical solutions to the existing challenges with transportation infrastructures such as accidents and congestion. However, the transition to the era of CAVs would be gradual, and it could be expected that both CAVs and human-driven vehicles (HDVs) would exist in the network for some time, which could change the fundamental properties of urban networks. In this paper, the impact of CAVs on macroscopic fundamental diagram (MFD) is analyzed with microscopic traffic simulations, and the sensitivity analysis of market penetration rates of CAVs and network configurations is conducted. The analysis shows that one-way grid networks offer the most accessible and resilient environment during various phases of CAV introduction. Moreover, the introduction of CAVs not only improves the aggregated network performance but also improves the accessibility (trip completion rate) of regular HDVs.**

I. INTRODUCTION

Connected and autonomous vehicles (CAVs) with capabilities such as shorter reaction time and tighter headways seem like a promising solution for current challenges with transportation infrastructures such as accidents and traffic congestion. With the recent advances in communication technology, the implementation of CAVs looks feasible in the near future. In some countries, such as the Netherlands, under certain conditions CAVs are allowed on public roads [1]. Considering their continuous sensing and almost instant reaction time advantage [2], CAVs can reduce human errors which have been the major cause of crashes [3]. In addition, their shorter reaction times result in closer spacing between vehicles so as to increases road capacities [2]. Moreover, CAV-enabled adaptive routing can lead to the optimal spread of vehicles in the network so as to reduces the risk of gridlock [4].

Ideally, in a fully connected and autonomous environment where 100% of vehicles are CAVs, no traffic signal or road signs would be required to operate transportation systems. However, removing all human-driven vehicles (HDVs) would not happen over a night, i.e., in the early stages of CAV development, CAVs and HDVs have to share roads. Therefore, proper planning for the transition process is important, specifically, in urban areas where limited space for road expansion is available. An existing study proved that even at low market penetration rates (MPRs), CAVs still can improve traffic stability and network throughput [5]. However, the impacts of network layout on network performance in the mixed environment of CAVs and HVs have not been well investigated.

This paper aims at studying the impacts of different MPRs of CAVs on the macroscopic fundamental diagram (MFD) of gird networks with common configurations (i.e. two-way, two-way with prohibited left turns, and one-way). This will aid policymakers to effectively plan for efficient use of the limited urban space and achieve the highest capacity throughout the transition to 100% CAVs. To quantitatively assess the impact, MFD relating the average network accumulation (number of vehicles inside the network) to network production (total distance travelled by vehicles per unit of time which is a measure of traffic flow) is utilized. MFD not only allows for network performance evaluation in an aggregated manner but also is independent of the traffic demand [6] which makes it appropriate for control applications. In this paper, CAVs with different MPRs are loaded to the same grid network with the same demand but with different network configurations (i.e., one-way, two-way, two-way with banned left turns) to discover the optimal network layout with the highest trip serving capacity and resiliency.

The rest of this paper is organized as follows. Section II reviews the related works to this study. Section III introduces the simulated network settings, vehicle types, and traffic scenarios. Section IV discusses the impact of CAVs on MFD resilience and network accessibility with microscopic traffic simulations. Finally, Section V concludes the findings of this paper and the recommendations for future research.

II. RELATED WORK

The research about macroscopic traffic monitoring can be traced back to the 1960s [7], [8]. However, it was not well investigated until the last decade when [9] suggested if the network is redundant, homogeneous, uniformly loaded, and minimally affected by turning vehicles, the average network flow (or production) is a function of network density (or occupancy). Later, [6] suggested the existence of the MFD by field data and showed that when the highly scattered link fundamental diagrams were aggregated, the scatters disappeared and points showed a clear relationship between network density and flow. Other studies empirically showed the existence of MFD by analyzing real traffic data for Brisbane Australia [10], Bern, Switzerland, London, UK, and

*Research was supported by Natural Sciences and Engineering Research Council of Canada (NSERC).

[1] Mohammad Halakoo is with the Department of Civil Engineering, McMaster University, L8S 4L8 Hamilton, Ontario, Canada.
Email: halakoom@mcmaster.ca

[2] Hao Yang is with the Department of Civil Engineering, McMaster University, L8S 4L8 Hamilton, Ontario, Canada.
Email: haoyang@mcmaster.ca
†Corresponding Author

2021 IEEE Intelligent Vehicles Symposium (IV) | 978-1-7281-5394-0/21/$31.00 ©2021 IEEE | DOI: 10.1109/IV48863.2021.9575687

Madrid, Spain [11]. [6] also showed that there was a direct relationship between the circulating flow and the outflow. This finding was important from the practical point of view, since measuring the outflow was a nontrivial task in practice while circulating flow could be easily measured by loop detectors. Therefore, MFD could be used for measuring trip completion rate and accessibility in the network. These unique characteristics also resulted in various applications of MFD for traffic management, such as perimeter control [12], safety evaluation [13], and planning implications [14], etc.
In the literature, various methods, including an analytical method based on variational theory [9], empirical method with local traffic measurements [15], and trajectory-based method, were used to calibrate MFD. [16] compared different methods for MFD calculation and concluded that the analytical MFD is the upper bound of empirical MFD.

Given the fact that MFD is a property of the network, some studies in the literature investigated the impacts of different network configurations on the MFD and trip serving capacities. [17] analytically compared the capacity of one-way and two-way networks and concluded that the average trip length was a significant factor to determine the trip serving capacity of the two networks. In the other words, when the trip lengths were short, the two-way layout resulted in higher trip completion and lower lost time, and one-way networks were offset by more circuity. Banning the left turns also led to higher trip serving in two-way networks even when trips were long. [18] investigated the impact of prohibiting left turns on improving urban network efficiency, and it showed that the benefit of left-turn movement prohibition on improving the efficiency of the network (considering network exit function (NEF) and MFD as proxies for that purpose) depended on the density of the network. When the network was loaded very lightly or extremely heavily, the prohibition of left turns did not increase the trip completion rate. Hence, they proposed for achieving the most efficient results, left turn accommodation policy should be based on the network accumulation. [19] studied the impacts of various grid network configurations, including two way (TW), two way with prohibited left turns (TWL), and one way (OW), on NEF. The study showed that the NEF flow for TW networks was smaller than OW and TWL, and the length of the left turn pocket was an effective factor in the performance of the TW networks, meaning TW networks with shorter left-turn pockets (5m) gridlocked faster than the longer (25m) ones. In addition, with a higher Kirchhoff parameter, TWL networks outperform in terms of average speed, delay and trip length which was attributed to the lack of redundant paths in TWL networks. Moreover, [14] studied the impact of link removal in a TW grid network on network performance indicators such as total travel time and showed that removing central links were more detrimental to network performance compared to peripheral link removal.

The literature also studied the impact of the technologies of connectivity and autonomy, from adaptive driving and routing to fully autonomous vehicles, on network efficiency indicators, such as trip completion rate and maximum throughout. [20] showed the provision of real-time information about the traffic condition (i.e., adaptive driving) could improve network trip completion rate by more than 10% when 100% adaptive driving was applied. However, the improvement from 30% to 100% adaptivity was very trivial, and more scatters were observed in the MFD. [5] studied the impact of CAVs on flow stability and throughput, and they found that at low MPRs, combining autonomy and connectivity could significantly increase flow stability. Moreover, increasing MPRs reduced the scatters of MFD and increased maximum throughput, and autonomous vehicles only contributed to higher throughput compared to connected vehicles at the same MPR. Moreover, [21] expanded the scope of studying the impact of CAVs from a highway segment to highway network in Antwerp, Belgium and showed that at high demand levels and higher MPR, CAVs' shorter gaps improved the network's average harmonic speed. [22] investigated the impact of autonomous vehicles (AVs) on the MFD of the idealized two-ring network. They concluded that the turning and merging behaviours of AVs had negative impacts on the stability of the network, and it was worsened as the probability of turn increased. In conclusion, they suggested that AVs without connectivity despite increasing network flow, due to their merging and turning maneuvers (even less frequent ones) led to increasing network instability.

The aforementioned review indicated that it was very challenging to understand the relationship between network configuration and network trip serving capacity under a mixed CAV and HDV environment. This paper will take the advantage of micro-simulation tools for modelling the behaviour of HDVs and CAVs to fill this gap.

III. Microscopic Simulation Analysis

To understand the impact of CAVs on MFD, especially network trip serving capacity, under different network configurations, a grid network is designed with a microscopic traffic simulator, Aimsun [23] that was used in the literature for simulating the mixed flow of HDVs and CAVs [21], [24]. Both HDVs and CAVs and their behaviours are modelled in the simulation. The settings of the networks, features of HDVs and CAVs, and simulation scenarios are described in the rest of this section.

A. Simulated Network

In this subsection, a 5X5 square grid network is designed, and Figure 1 shows the geometry of the network. The lengths of all links are set as 200 meters, and 60 centroids are placed in the middle of the links to emulate trip generation/ attraction along the route [19].

The capacity of each lane is set as 900 vph. In the simulation, all links of the OW network are modelled as two-lane sections, while they are set as one-lane links in each direction for both TW and TWL networks. In addition, for the TW network, 20m left-turn pockets are considered, and their speed limit is set to 50 km/h.

Moreover, the network is loaded with a uniform demand (30,000 veh in total), which gradually increases during the first hour and keeps constant in the second hour. To allow the network to recover from congestion, no vehicles are added to the network in the third hour. The demand profile is shown in

Figure 2Figure 2. Aimsun dynamic traffic assignment module with logit model (with scale parameter 1) is applied for trip assignment. The costs of links are updated every 5 minutes for route choices.

In addition, all intersections are controlled by fixed time signals with a cycle length of 60 s and a yellow time of 2 s. In the TW network, the four-legged intersections are controlled with four phases: two through movements and right turns (20 s), and two protected left turns (6 s). The three-legged intersections are controlled with three phases in the TW network: through movement and right turn (20 s), protected left turn (6 s), and right and left turns from the perpendicular link (26 s). In the TWL and OW network, a simple two-phase signal (two through and right-turn movements 28 s) is applied. All three-legged intersections in TWL and OW networks are modelled as yellow boxes, with which vehicles do not enter the intersection unless there is enough gap ahead.

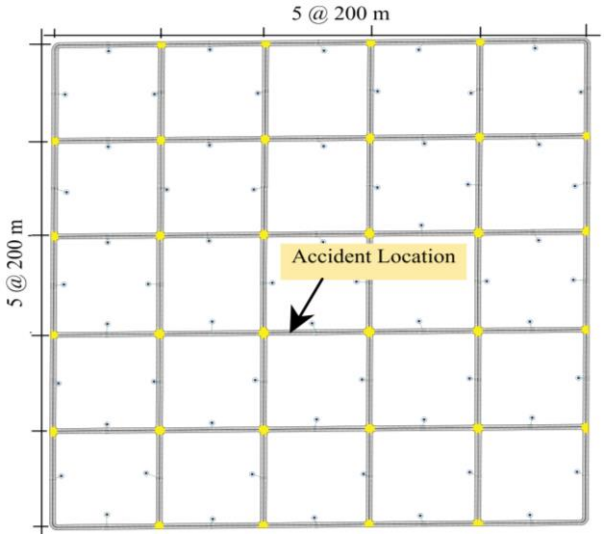

Figure 1 Simulated network and accident

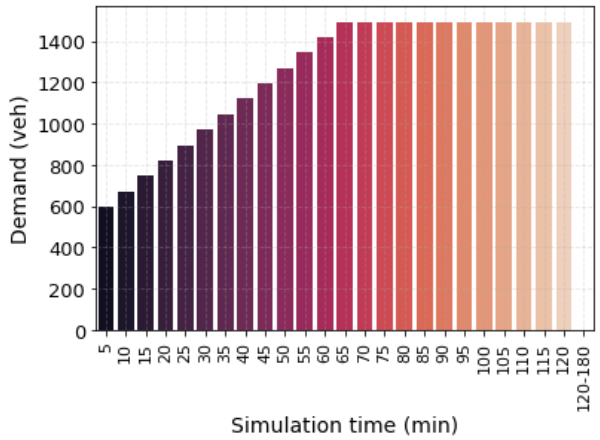

Figure 2 Simulated demand profile

B. *Features of HDVs and CAVs*

This subsection describes the behaviours of both HDVs and CAVs simulated Aimsun. Three distinct features of HDVs and CAVs are described, including their deterministic behaviour, real-time routing, and shorter reaction time. Table I summarizes the parameter values for the two types of vehicles.

In the simulation, both HDVs and CAVs are modelled based on the Gipps car-following model, the default car following model in Aimsun. The reaction time of CAVs is set as 0.2 s and 0.8 s for HDVs. This idea is based on [24] approach for modelling AVs which assumed that they drive sufficiently similar to HDVs only with some enhanced competencies such as shorter reaction time. Also, the minimum clearance at stop is reduced from 1 m for HDVs to 0.5 m for CAVs (similar to [25], [26]). The settings allow CAVs to quickly respond to the changes of traffic on roads as well as to maintain a closer gap with their leaders. In addition, the stochasticity in parameters, such as minimum/maximum acceleration/deceleration, speed limit acceptance, is removed from CAVs to allow them to have accurate control of dynamics [24]. Moreover, the cooperative adaptive cruise control (CACC) is deployed by CAVs, and the maximum platoon size is set as 10 vehicles.

For routing behaviours, both HDVs and CAVs implement dynamic user equilibrium (DUE), and the results are saved as a path assignment for all designed experiments. In addition, the CAVs are marked as en-route vehicles, which can change their route after assignment to a route, while HDVs follow the path being assigned at their entry based on the recently updated link travel time. Moreover, the distribution of CAVs in each origin-destination (OD) pair is assumed to be uniform, i.e., the numbers of HDVs and CAVs are determined based on the defined MPRs.

Table I Comparison of HDV and CAV features

Feature (unit)	HV	CAV
Reaction time (s)	0.8	0.2
Reaction time at stop (s)	1.2	0.2
Reaction time for vehicle ahead of queue (s)	1.6	0.2
Platoon size (veh)	-	10
Speed limit acceptance	1.1	1
Maximum desired speed (km/h)	110	110
Maximum acceleration (m/s^2)	3	3
Normal deceleration (m/s^2)	4	4
Maximum deceleration (m/s^2)	6	6
Clearance (m)	1	0.5
Sensitivity factor	1	1
Vehicle length (m)	4	4
Speed gain	-	0.0125
Distance gain (s^{-1})	-	0.45
Time gap leader (s)	-	1.5
Time gap follower (s)	-	0.6
Lower gap threshold (s)	-	1.5
Higher gap threshold (s)	-	2
Assignment method	DUE (Logit)	DUE (Logit)
Update cycle for routing information (min)	5	5
En-route percentage (%)	0	100

C. *Simulation Scenarios*

In this paper, the impact of MPRs of CAVs on MFD will be analyzed to understand the changes in network properties at different stages of CAV development. In the simulation, three different MPRs of CAVs (20%, 50%, 80%) are modelled with the same demand under three grid network configurations (OW, TW, TWL). In the analysis, traffic information,

including link flow and density and completed trip rates, is collected every minute.

For the estimation of MFD, the trip production (vehicle-km/min), which is the sum of all distance travelled in the network, and the number of vehicles inside the network (veh) are calculated at every minute [27]. Also, for comparing the resiliency of different network configurations in handling disruptions of road events, an incident closing one lane in the center of the network is modelled. The length of the incident is 6 meters, and it is active during [60, 105] minutes. Also, no accident broadcasting or roadside units are simulated to inform the users. Nonetheless, the CAVs are able to adapt their route to avoid the affected links based on updated path travel time. Note that since this paper focuses on understanding MFD at mixed CAV and HDV environments, the scenario with 100% MPR will not be discussed.

IV. Results and Discussion

In this section, the results in the aforementioned traffic scenarios are discussed to understand MFD at different MPRs of CAVs and network configurations. The resilience of the network and vehicle accessibility are also discussed.

A. MFDs of Grid Networks

Figure 3 (A)-(D) show the MFD from four different MPRs of CAVs (0%, 20%, 50%, 80%) under three network configurations without deploying the incident, while Figure 3 (E)-(H) illustrate the other four scenarios with the incident. The figures demonstrate that increasing MPRs of CAVs results in higher network capacities and this can be explained by shorter reaction time and a smaller minimum clearance of CAVs. Moreover, the OW network offers the highest capacity followed by the TWL network, and TW being the worst. In the simulation, the MFD from the OW network only shows the free-flow state (even with accident), while the other two networks gridlock when the accident happens despite having the same demand levels.

Moreover, when there is no incident, the capacity difference between the OW and TWL networks decreases at higher MPRs, which indicates the support of real-time routing with CAVs can increase network mobility. However, when the MPR reaches 80%, the standard deviation of density in the TWL network reaches its highest value and around 400 vehicles are still in the network while network production is zero which suggests some parts of the network are gridlocked (see Figure 3 (D) and Figure 4 (D)). Also, the congested branch of MFD in the TW network looks oscillatory at MPR=80% which indicates the instability of the network. Capacity improvement in the OW might seem to decrease at higher MPRs. However, it can be seen that with the increase in MPRs, the critical accumulation decreases while production either remains the same or increases which indicates that network capacity is increased. In this case, since the demand was not large enough, the network recovers before reaching its new higher capacity. The capacity of the intersections is significantly higher in OW and TWL networks due to more green time (28 s vs 20 s) and less lost time (4 s vs 8 s) compared to the TW network. Therefore, OW and TWL networks demonstrate higher production values compared to the TW network.

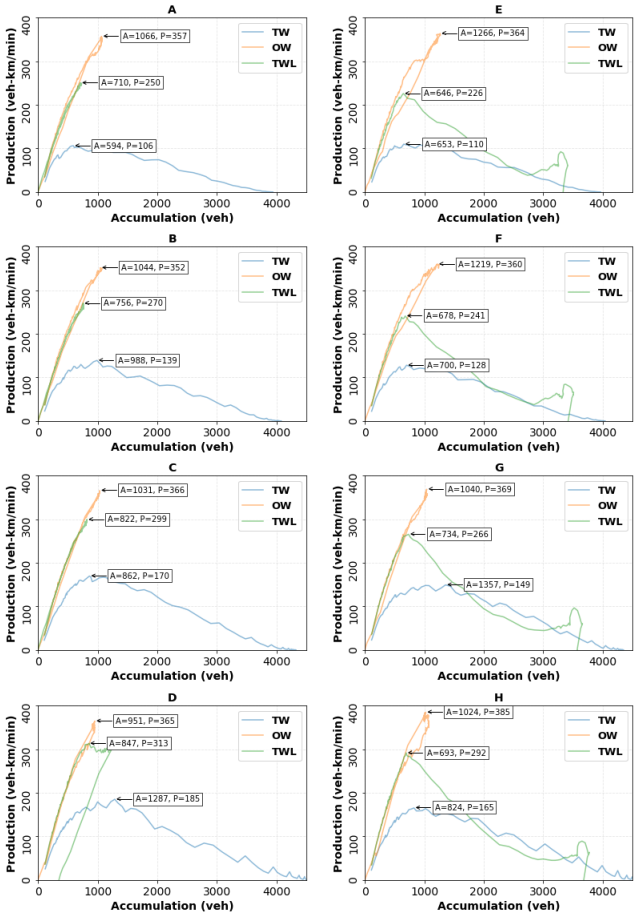

Figure 3 Network MFD: A(0% MPR No accident), B(20% MPR No Accident), C(50% No Accident), D(80% MPR No Accident), E(0% MPR With Accident), F(20% MPR With Accident), G(50% MPR With Accident), H(80% MPR With Accident)

B. Hysteresis Loops and Resilience

In this subsection, the hysteresis of MFD and the resilience of the network are evaluated. In transportation networks, hysteresis loops are caused during the loading and recovery of the network when the congestion is unevenly distributed [4]. The area inside the hysteresis loop shows network congestion dissipation and gridlock recovery, i.e., the smaller the area the faster recovery from gridlock [28].

Figure 3 shows that the hysteresis loop size in the OW network is considerably smaller than the other two networks i.e., the OW network can better recover from congestion. This can be explained by the higher path redundancy in the OW network. With that, the OW network can recover from congestion faster and generate a smaller loop area, while the other two networks are gridlocked. The result is similar to the study in [19]. In addition, according to [14], in symmetric grid networks with uniform demand, the majority of the flow is concentrated in the center. In that sense, if a central link is temporarily closed by an incident during a busy time, which is also the most disruptive scenario in a grid network, the network with high path redundancy, i.e., the OW network, can minimize the impact of the incident with the alternative

shortest paths, and higher MPRs of CAVs can better take advantage of the redundancy, which explains the smaller hysteresis loop size. Moreover, when the MPR increases from 50% to 80%, the hysteresis loop of MFD in the OW network slightly expands, which implies the homogeneity of congestion is slightly decreased. The other two networks also show a similar pattern. This observation can be attributed to the extra turning maneuvers that are caused by adaptive routing. It is anticipated that this issue can be resolved if either more advanced signal control strategies or finely tuned routing parameters are applied.

The multi-valuedness in the right tail of MFD with an accident in TWL networks (see Figure 3 (F)-(H)) indicates this network is not completely gridlocked and some vehicles still have mobility. This is the result of the uneven distribution of congestion during the recovery and loading process. Increasing MPRs of CAVs can push this multi-valuedness point to the right, which means the network can sustain higher density, i.e., the network has higher resilience.

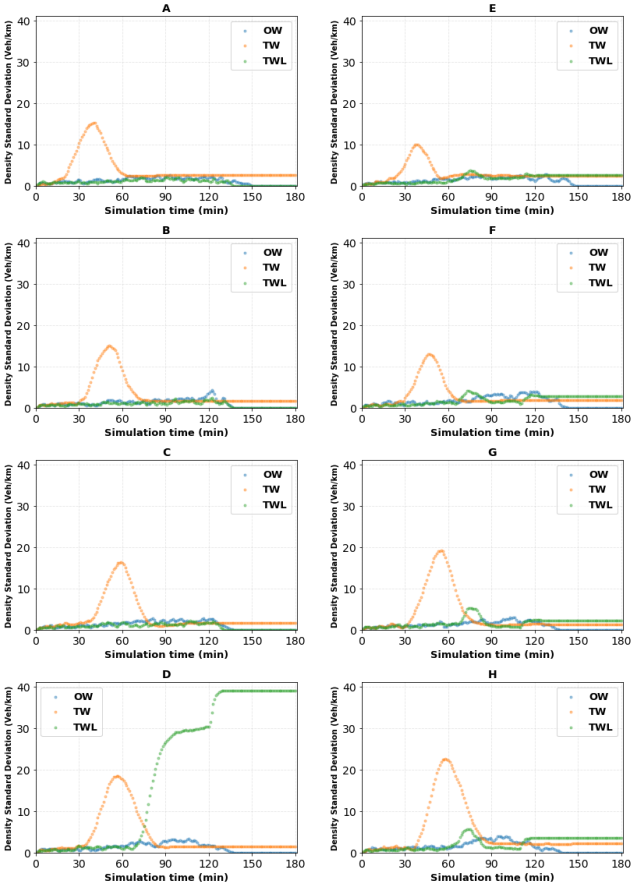

Figure 4 Network Density Standard Deviation: A(0% MPR No accident), B(20% MPR No Accident), C(50% No Accident), D(80% MPR No Accident), E(0% MPR With Accident), F(20% MPR With Accident), G(50% MPR With Accident), H(80% MPR With Accident)

C. *Accessibility*

In this subsection, the network accessibility is evaluated with the simulations. The accessibility can be measured with the trip completion rate [6]. It has been demonstrated that the OW network with higher shortest path redundancy has higher trip completion rates [14], and the production in MFD is highly correlated to the rate [27]. Hence, the system accessibility improvement is larger in the OW network with higher MPR. Nevertheless, the accessibility benefit to HDVs is not well investigated.

Figure 5 shows the trip completion rates (the value is normalized by dividing MPRs of HDVs) under different MPRs and network configurations. The figure verifies that the accessibility for HDVs can be increased at higher CAV MPRs. However, the benefit is considerable for the OW and TW networks with and without incident. While the TWL network gains insignificant accessibility improvement at higher MPRs, the occurrence of an accident slightly highlights the benefits, especially at high MPRs. The result demonstrates the accessibility benefits of connectivity and autonomy on both CAVs and HDVs under different network configurations. In conclusion, the accessibility improvement for HDVs with higher MPRs is more pronounced in the TW network.

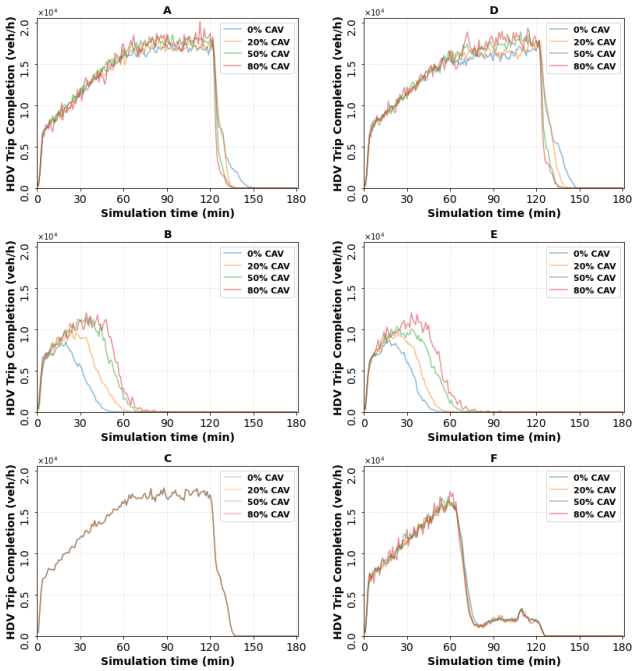

Figure 5 HDV Trip Completion: A (OW, No Accident), B (TW, No Accident), C (TWL, No Accident), D (OW, With Accident), E (TW, With Accident), F (TWL, With Accident)

V. Conclusions

In this paper, the effect of network configures under different MPRs of CAVs on urban network performance was investigated. The results showed that the capacity and resilience of the network to disruption increased at higher MPRs of CAVs. Also, the OW network brought up more benefits (i.e., higher accessibility and capacity as well as a better response to disruptions). In addition, the accessibility of HDVs throughout increasing MPRs was discussed. The results showed that the increasing MPR not only benefited CAVs but also improved accessibility for HDVs. Especially, when disruption happens, the benefits were more pronounced. In general, the results suggested the OW network worked the best throughout the transition of transportation from the

existing situation to the fully connected and autonomous environment.

Based on the findings in this paper, there are some recommendations for future work. First, this paper only investigated a fixed time control plan for a grid network for the sake of simplicity. The study of the transition process to connected and autonomous environments with more advanced traffic control systems and vehicle to infrastructure (V2I) communication will be conducted to more accurately understand the benefits of CAVs. Moreover, a sensitivity analysis of demand levels and patterns (e.g., directional demand) will be conducted to understand the impact of CAVs on MFD at different congestion levels. Also, the effects of the locations and types of incidents will be investigated in the future. In this study, Aimsun microscopic simulator was used but the replication and comparison of results with other simulators such as VISSIM and SUMO will be investigated in the future.

Last but not least, due to the limited implementation of CAVs at the time of writing this paper, the experiments are all done in the simulated environment. Apparently, the replication of the experiment with real CAVs would be an interesting topic for future works.

REFERENCES

[1] KPMG, "2019 Autonomous Vehicles Readiness Index: Assessing countries' preparedness for autonomous vehicles," p. 60, 2019, [Online]. Available: https://assets.kpmg/content/dam/kpmg/xx/pdf/2019/02/2019-autonomous-vehicles-readiness-index.pdf.

[2] H. S. Mahmassani, "50th Anniversary invited article autonomous vehicles and connected vehicle systems: Flow and operations considerations," *Transp. Sci.*, vol. 50, no. 4, pp. 1140–1162, 2016, doi: 10.1287/trsc.2016.0712.

[3] D. J. Fagnant and K. Kockelman, "Preparing a nation for autonomous vehicles: opportunities, barriers and policy recommendations," *Transp. Res. Part A Policy Pract.*, vol. 77, pp. 167–181, 2015.

[4] C. F. Daganzo, V. V. Gayah, and E. J. Gonzales, "Macroscopic relations of urban traffic variables: Bifurcations, multivaluedness and instability," *Transp. Res. Part B Methodol.*, vol. 45, no. 1, pp. 278–288, 2011, doi: 10.1016/j.trb.2010.06.006.

[5] A. Talebpour and H. S. Mahmassani, "Influence of connected and autonomous vehicles on traffic flow stability and throughput," *Transp. Res. Part C Emerg. Technol.*, vol. 71, pp. 143–163, Oct. 2016, doi: 10.1016/j.trc.2016.07.007.

[6] N. Geroliminis, C. F. Daganzo, and N. Geroliminis, "Existence of urban-scale macroscopic fundamental diagrams: Some experimental findings," *Transp. Res. Part B Methodol.*, vol. 42, no. 9, pp. 759–770, 2008, doi: 10.1016/j.trb.2008.02.002.

[7] J. G. Wardrop, "Journey speed and flow in central urban areas," *Traffic Eng. Control*, vol. 8, no. 8, 1968.

[8] J. W. Godfrey, "The mechanism of a road network," *Traffic Eng. Control*, vol. 8, no. 8, 1969.

[9] C. F. Daganzo and N. Geroliminis, "An analytical approximation for the macroscopic fundamental diagram of urban traffic," *Transp. Res. Part B Methodol.*, vol. 42, no. 9, pp. 771–781, 2008, doi: 10.1016/j.trb.2008.06.008.

[10] T. Tsubota, A. Bhaskar, and E. Chung, "Macroscopic Fundamental Diagram for Brisbane, Australia," *Transp. Res. Rec. J. Transp. Res. Board*, vol. 2421, no. 1, pp. 12–21, 2014, doi: 10.3141/2421-02.

[11] A. Loder, L. Ambühl, M. Menendez, K. W. Axhausen, M. Verità, and / Ascona, "Network features and MFD parameters," 2017, [Online]. Available: http://www.strc.ch/2017/Loder_EtAl.pdf.

[12] M. Keyvan-Ekbatani, A. Kouvelas, I. Papamichail, and M. Papageorgiou, "Exploiting the fundamental diagram of urban networks for feedback-based gating," *Transp. Res. Part B Methodol.*, vol. 46, no. 10, pp. 1393–1403, 2012, doi: 10.1016/j.trb.2012.06.008.

[13] R. Alsalhi, V. V. Dixit, and V. V. Gayah, "On the existence of network macroscopic safety diagrams: Theory, simulation and empirical evidence," *PLoS One*, vol. 13, no. 8, pp. 1–20, 2018, doi: 10.1371/journal.pone.0200541.

[14] J. Ortigosa and M. Menendez, "Traffic performance on quasi-grid urban structures," *Cities*, vol. 36, pp. 18–27, 2014, doi: 10.1016/j.cities.2013.08.006.

[15] C. Buisson and C. Ladier, "Exploring the impact of homogeneity of traffic measurements on the existence of macroscopic fundamental diagrams," *Transp. Res. Rec.*, no. 2124, pp. 127–136, 2009, doi: 10.3141/2124-12.

[16] T. Courbon and L. Leclercq, "Cross-comparison of macroscopic fundamental diagram estimation methods," *Procedia - Soc. Behav. Sci.*, vol. 20, pp. 417–426, 2011, doi: 10.1016/j.sbspro.2011.08.048.

[17] V. Gayah and C. Daganzo, "Analytical capacity comparison of one-way and two-way signalized street networks," *Transp. Res. Rec.*, no. 2301, pp. 76–85, 2012, doi: 10.3141/2301-09.

[18] A. J. Deprator, O. Hitchcock, and V. V. Gayah, "Improving urban street network efficiency by prohibiting conflicting left turns at signalized intersections," *Transp. Res. Rec.*, vol. 2622, no. 1, pp. 58–69, 2017, doi: 10.3141/2622-06.

[19] J. Ortigosa, M. Menendez, and V. V Gayah, "Analysis of network exit functions for various urban grid network configurations," *Transp. Res. Rec.*, vol. 2491, no. 1, pp. 12–21, 2015.

[20] M. Saberi, H. S. Mahmassani, and A. Zockaie, "Network capacity, traffic instability, and adaptive driving: findings from simulated urban network experiments," *EURO J. Transp. Logist.*, vol. 3, no. 3–4, pp. 289–308, 2014, doi: 10.1007/s13676-013-0040-2.

[21] M. Makridis, K. Mattas, B. Ciuffo, M. A. Raposo, T. Toledo, and C. Thiel, "Connected and automated vehicles on a freeway scenario. Effect on traffic congestion and network capacity," *7th Transp. Res. Arena*, no. April, p. 13, 2018, doi: 10.5281/zenodo.1483132.

[22] Z. Gu and M. Saberi, "Effects of Turning and Merging on Network Traffic Instability: A Simulation-Based Analysis of Human-Driven and Autonomous Vehicles," *CoRR*, vol. abs/1904.1, 2019, [Online]. Available: http://arxiv.org/abs/1904.11677.

[23] TTS, "Aimsun 8 Users ' Manual July 2014 © 2005-2014 TSS-Transport Simulation Systems," *TSS-Transport Simul. Syst.*, no. July, 2014.

[24] A. Kouvelas, J. P. Perrin, S. Fokri, and N. Geroliminis, "Exploring the impact of autonomous vehicles in urban networks and potential new capabilities for perimeter control," *5th IEEE Int. Conf. Model. Technol. Intell. Transp. Syst. MT-ITS 2017 - Proc.*, pp. 19–24, 2017, doi: 10.1109/MTITS.2017.8005671.

[25] Atkins, "Research on the Impacts of Connected and Autonomous Vehicles (CAVs) on Traffic Flow," 2016.

[26] Q. Lu, T. Tettamanti, D. Hörcher, and I. Varga, "The impact of autonomous vehicles on urban traffic network capacity: an experimental analysis by microscopic traffic simulation," *Transp. Lett.*, vol. 00, no. 00, pp. 1–10, 2019, doi: 10.1080/19427867.2019.1662561.

[27] N. Geroliminis and C. F. Daganzo, "Macroscopic modeling of traffic in cities," *TRB 86th Annu. Meet.*, no. January, pp. 07–0413, 2007, [Online]. Available: http://www.ce.berkeley.edu/~nikolas/RESUME_files/07-0413.pdf.

[28] F. Fakhrmoosavi, R. Saedi, A. Zockaie, and A. Talebpour, "Impacts of Connected and Autonomous Vehicles on Traffic Flow with Heterogeneous Drivers Spatially Distributed over Large-Scale Networks," *Transp. Res. Rec. J. Transp. Res. Board*, vol. 2674, no. 10, pp. 817–830, 2020, doi: 10.1177/0361198120940997.